Title

A receptor-like protein mediates plant immune responses to herbivore-associated molecular patterns

Journal

Proceedings of the National Academy of Sciences of the United States of America, 117(49)

ISSN

0027-8424

Authors

Steinbrenner, Adam D
Muñoz-Amatriaín, Maria
Chaparro, Antonio F
et al.

Publication Date

2020-12-08

DOI

10.1073/pnas.2018415117

Peer reviewed

A receptor-like protein mediates plant immune responses to herbivore-associated molecular patterns

Adam D. Steinbrenner[a,b,1], Maria Muñoz-Amatriaín[c,d], Antonio F. Chaparro[b], Jessica Montserrat Aguilar-Venegas[a,e], Sassoum Lo[c], Satohiro Okuda[f], Gaetan Glauser[g], Julien Dongiovanni[g], Da Shi[h], Marlo Hall[a], Daniel Crubaugh[a], Nicholas Holton[i], Cyril Zipfel[i,j], Ruben Abagyan[h], Ted C. J. Turlings[g], Timothy J. Close[c], Alisa Huffaker[a], and Eric A. Schmelz[a,1]

[a]Section of Cell and Developmental Biology, Division of Biological Sciences, University of California San Diego, La Jolla, CA 92093; [b]Department of Biology, University of Washington, Seattle, WA 98195; [c]Department of Botany and Plant Sciences, University of California, Riverside, CA 92521; [d]Department of Soil and Crop Sciences, Colorado State University, Fort Collins, CO 80523; [e]Laboratory of AgriGenomic Sciences, Escuela Nacional de Estudios Superiores Unidad Leon, Universidad Nacional Autonoma de Mexico, 37684 Leon, Mexico; [f]Department for Botany and Plant Biology, University of Geneva, CH-1211 Geneva, Switzerland; [g]Institute of Biology, University of Neuchâtel, 2000 Neuchâtel, Switzerland; [h]Skaggs School of Pharmacy and Pharmaceutical Sciences, University of California San Diego, La Jolla, CA 92093; [i]The Sainsbury Laboratory, University of East Anglia, NR4 7UH Norwich, United Kingdom; and [j]Department of Plant and Microbial Biology, Zürich-Basel Plant Science Center, University of Zürich, CH-8008 Zürich, Switzerland

Edited by Sheng Yang He, Duke University, and approved October 23, 2020 (received for review September 2, 2020)

Herbivory is fundamental to the regulation of both global food webs and the extent of agricultural crop losses. Induced plant responses to herbivores promote resistance and often involve the perception of specific herbivore-associated molecular patterns (HAMPs); however, precisely defined receptors and elicitors associated with herbivore recognition remain elusive. Here, we show that a receptor confers signaling and defense outputs in response to a defined HAMP common in caterpillar oral secretions (OS). Staple food crops, including cowpea (*Vigna unguiculata*) and common bean (*Phaseolus vulgaris*), specifically respond to OS via recognition of proteolytic fragments of chloroplastic ATP synthase, termed inceptins. Using forward-genetic mapping of inceptin-induced plant responses, we identified a corresponding leucine-rich repeat receptor, termed INR, specific to select legume species and sufficient to confer inceptin-induced responses and enhanced defense against armyworms (*Spodoptera exigua*) in tobacco. Our results support the role of plant immune receptors in the perception of chewing herbivores and defense.

herbivory | LRR-RLP | PRR | HAMP | receptor

The global balance between autotroph and heterotroph biomass is dictated by a nearly immeasurable number of plant–herbivore interactions. Similarly, historic pest challenges and modern herbivore invasions still threaten global food security (1–3). Plant resilience in both natural and agricultural settings is mediated by inducible biochemical defenses against herbivores. Importantly, the nature and magnitude of plant responses are often amplified by specific biochemical elicitors, termed herbivore-associated molecular patterns (HAMPs), associated with attackers (4, 5). Despite the critical need for a mechanistic understanding of induced defense responses, specific receptors perceiving HAMPs have remained elusive (6).

Plants can specifically perceive Lepidopteran herbivores by sensing HAMPs in oral secretions (OS) (7, 8). Among defense-eliciting molecular patterns, inceptins are a potent bioactive series of proteolytic fragments derived from host chloroplastic ATP synthase γ-subunit (cATPC) and found in the OS of all examined Lepidopteran species (8–10). The dominant inceptin present during caterpillar herbivory on cowpea (*Vigna unguiculata*) is an 11-amino acid (AA) peptide, termed *Vu*-In ($^{+}$ICDINGVCVDA^{-}). The *Vu*-In epitope is highly conserved among plant cATPC sequences; however, only species within the legume subtribe Phaseolinae respond to inceptins (11).

In plants, both nonself and modified-self extracellular peptide signals can be recognized by specific pattern recognition receptors (PRRs) (12, 13). We hypothesized that legumes encode an inceptin receptor (INR) enabling *Vu*-In recognition, analogous to perception of pathogen-associated molecular patterns (PAMPs) by receptor kinases (RKs) and receptor-like proteins (RLPs) (12, 14). Here, we identify and characterize closely related RLP-encoding genes from legumes in subtribe Phaseolinae that confer signaling and defense outputs in response to specific HAMP elicitors found in caterpillars.

Results

To identify INR candidates, we examined plant response variation to both *Vu*-In and a less bioactive C-terminal truncated inceptin, termed *Vu*-In^{-A} ($^{+}$ICDINGVCVD^{-}), found in the OS of a legume specialist herbivore (*Anticarsia gemmatalis*) (10). Anticipating an arms race pattern of evasion and reestablishment consistent with other elicitors (15, 16), we screened cowpea germplasm for positive *Vu*-In^{-A}–elicited responses. Accessions Danila, Suvita, and Yacine displayed induced ethylene production after applying *Vu*-In^{-A} to wounded leaves while other accessions failed to respond (Fig. 1*A*). Although responses to *Vu*-In^{-A} were quantitatively low compared to fully active *Vu*-In (Fig. 1*A*), we reasoned that the existence of qualitative response variation to

Significance

Plants respond to biotic attack using an immune system of receptors to recognize molecules associated with danger. We identified an immune receptor, termed inceptin receptor (INR), able to confer responses to defined inceptin peptide fragments present in caterpillar oral secretions. Like many plant immune receptors, INR is encoded only by certain plant species but can be transferred across families to confer new signaling and defense functions. While INR is only found in the genomes of cowpea, common bean, and related legumes, it confers defined elicitor responses to transgenic tobacco and suppresses the growth of attacking beet armyworm larvae. INR expands the breadth of plant pattern recognition receptors to detection of chewing insect herbivores.

Author contributions: A.D.S., C.Z., R.A., T.C.J.T., T.J.C., A.H., and E.A.S. designed research; A.D.S., M.M.-A., A.F.C., J.M.A.-V., S.L., S.O., G.G., J.D., D.S., M.H., D.C., and E.A.S. performed research; A.D.S., M.M.-A., A.F.C., J.M.A.-V., S.L., N.H., T.J.C., A.H., and E.A.S. contributed new reagents/analytic tools; A.D.S., M.M.-A., and E.A.S. analyzed data; and A.D.S. and E.A.S. wrote the paper.

The authors declare no competing interest.

This article is a PNAS Direct Submission.

See online for related content such as Commentaries.

[1]To whom correspondence may be addressed. Email: astein10@uw.edu or eschmelz@ucsd.edu.

This article contains supporting information online at https://www.pnas.org/lookup/suppl/doi:10.1073/pnas.2018415117/-/DCSupplemental.

First published November 23, 2020.

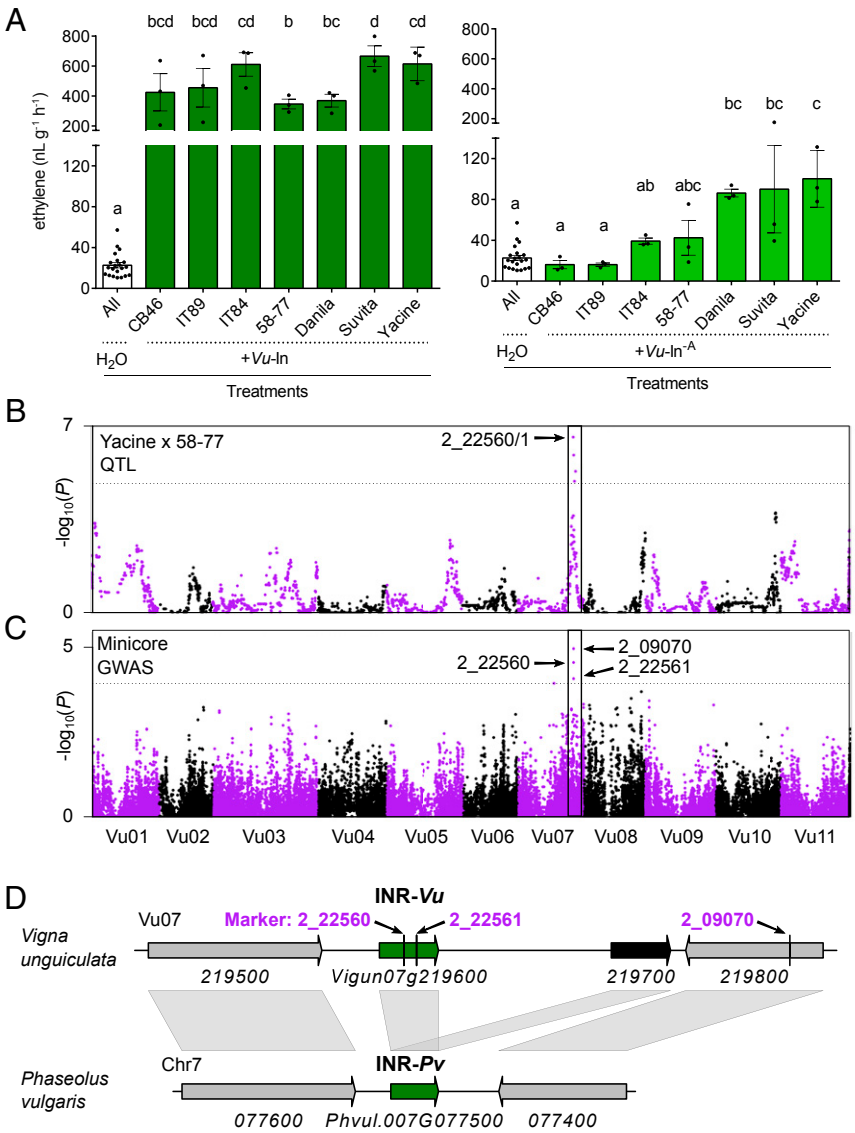

Fig. 1. Cowpea responses to an inceptin peptide associate with a single genetic locus. (*A*) Ethylene production in cowpea accessions after treatment with H_2O or 1 μM inceptin peptides. Bars show means ± SEM of replicate leaflets for individual inceptin treatments ($n = 3$) and all combined respective H_2O controls with label "All" ($n = 21$). Different letters represent significant differences (All ANOVAs $P < 0.05$; Tukey honestly significant difference [HSD], $\alpha = 0.05$). (*B*) QTL statistics for ethylene production ratio, *Vu*-In^{-A}/H_2O, in the Yacine × 58-77 RIL population. The dotted line indicates false discovery rate (FDR) significance cutoff (17,638 SNPs; modified Bonferroni correction at $\alpha = 0.05$) (*C*) Manhattan plot of GWAS results for ethylene production ratio, *Vu*-In^{-A}/H_2O, in 364 cowpea Minicore accessions. The dotted line indicates FDR cutoff at $\alpha = 0.05$ for 42,686 SNPs assigned respective physical coordinates in the cowpea genome (19). (*D*) Genomic region of chromosome 7 (Vu07; positions 34,220,090 to 34,258,839) containing highly associated marker SNPs (2_22560/1) and syntenic genes on common bean chromosome 7. Green and black filled arrows indicate LRR-RLP encoding genes.

the weaker elicitor variant could be mediated by *INR* genetic variation.

To map *INR*, we used a biparental population of 85 recombinant inbred lines (RILs) derived from a cross between accessions Yacine (*Vu*-In^{-A}–responsive) and 58–77 (*Vu*-In^{-A}–unresponsive) (Fig. 1*A*) for quantitative trait locus (QTL) mapping, as well as a panel of 364 cowpea accessions belonging to the University of California, Riverside (UCR) Minicore collection for a genome-wide association study (GWAS) (17). *Vu*-In^{-A} elicited variable ethylene production across accessions (*SI Appendix*, Fig. S1 and Tables S1 and S2). Using QTL mapping and GWAS, we observed that *Vu*-In^{-A} responses strongly associated with a single genetic locus in both populations (Fig. 1 *B* and *C* and *SI Appendix*, Fig. S2). In contrast to qualitative variation in plant responses to *Vu*-In^{-A}, quantitative variation in response to *Vu*-In resulted in different candidate loci that did not meet statistical thresholds for coassociation between QTL and GWAS efforts (*SI Appendix*, Fig. S2), were less well supported, and thus were not pursued further. The most highly associated markers with *Vu*-In^{-A} response in both QTL mapping and GWAS were single-nucleotide polymorphisms (SNPs) 2_22560, 2_22561, and 2_09070 (18), spanning a 22-kilobase (kb) region on chromosome 7 (Fig. 1*D* and *SI Appendix*, Fig. S1). Both markers 2_22560 and 2_22561 fell within an RLP-encoding gene *Vigun07g219600*, consistent with a potential role in receptor-mediated inceptin responses.

To examine function of the INR candidate, we transiently expressed *Vigun07g219600* from the reference accession IT97K-499-35 (19) in *Nicotiana benthamiana* and tested responsiveness to *Vu*-In. Hallmarks of receptor-mediated defense responses

include a burst of reactive oxygen species (ROS) and ethylene production. As a positive control, transient expression of the *EF*-Tu receptor (EFR) (20) in *N. benthamiana* conferred responses to elf18 peptide, but not *Vu*-In (Fig. 2*A*). Expression of *Vigun07g219600* selectively conferred *Vu*-In–induced ROS (Fig. 2 *B* and *C*) and ethylene production (Fig. 2*D*) to *Vu*-In, but not elf18, supporting the hypothesis that *Vigun07g219600* encodes a functional INR.

To understand the basis of phenotypic variation in cowpea, we cloned and expressed *INR* alleles from six accessions with differential *Vu*-In^{-A} responses (*SI Appendix*, Table S2). *Vu*-In^{-A} response variation originally observed in cowpea corresponded with *INR* allelic strength as only *INR* alleles from *Vu*-In^{-A}–responsive cowpea accessions conferred significant *Vu*-In–induced ROS and ethylene production in *N. benthamiana* (Fig. 2*E* and *SI Appendix*, Figs. S3 and S4). Both active and inactive RLP variants tagged with GFP colocalized with the plasma membrane marker PIP2A-mCherry (*SI Appendix*, Fig. S5). Interestingly, none of the tested alleles conferred *Vu*-In^{-A} responses in *N. benthamiana* (*SI Appendix*, Fig. S4). Given that all 364 tested cowpea accessions respond to *Vu*-In (*SI Appendix*, Table S1), our data support a model where cowpea natural variation in INR specifies an activation threshold for the weak elicitor, *Vu*-In^{-A}. When expressed heterologously in *N. benthamiana*, the same allelic series cannot confer responses to *Vu*-In^{-A} but is instead differentially activated by the stronger *Vu*-In elicitor (*SI Appendix*, Fig. S6).

INR is a leucine-rich repeat (LRR)-RLP, a receptor class distinguished from LRR-RKs by lack of an intracellular kinase domain (13). It contains 29 semiregular LRRs with intervening motif, preceding a transmembrane domain and short cytosolic segment (*SI Appendix*, Fig. S7). The *INR* locus in cowpea contains a paralog *Vigun07g219700* (72% AA similarity) that is unable to confer *Vu*-In–induced ethylene production when expressed in *N. benthamiana* (*SI Appendix*, Fig. S8). In contrast, orthologs with >90% AA similarity, *Phvul.007G077500* (from *Phaseolus vulgaris*) and *Vradi08g18340* (from *Vigna radiata*), conferred *Vu*-In–induced ethylene production (*SI Appendix*, Fig. S8). Notably, genome-sequenced *P. vulgaris* accession G19833 contains a single RLP receptor at the *INR* locus (Fig. 1*D*) and responds robustly to inceptin (*SI Appendix*, Fig. S9), excluding a strict requirement for duplicated receptor genes in responsive varieties. In more distantly related soybean (*Glycine max*), four syntenic homologs share 73 to 76% similarity to cowpea INR-*Vu* (*SI Appendix*, Fig. S7). Neither of two tested soybean homologs (*Glyma.10G228000*

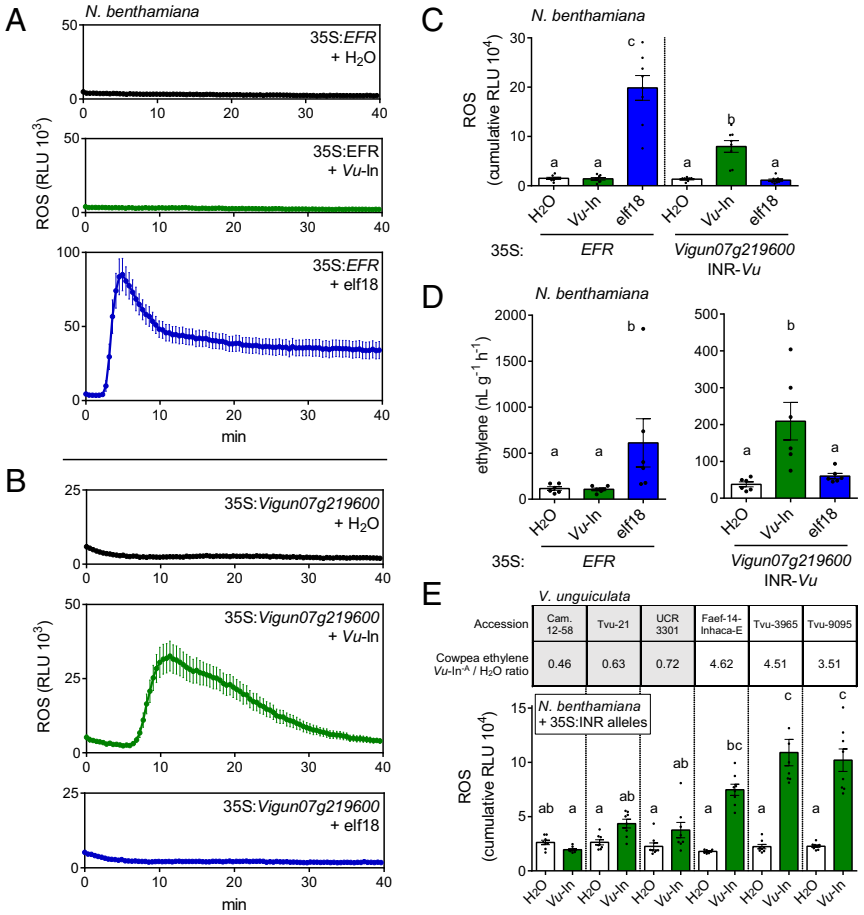

Fig. 2. INR confers inceptin signaling responses in heterologous model *N. benthamiana,* corresponding with cowpea response variation. (*A*–*C*) Ligand-dependent ROS production following the heterologous expression of receptors in *N. benthamiana*. Shone are relative luminescence units (RLU), minutes (min) after treatment with H_2O or 1 μM peptides elf-18 or *Vu*-In. (*A*) Peptides applied to plants expressing elf-18 receptor (elongation factor-Tu; EFR). (*B*) Peptides applied to plants expressing INR (INR-*Vu*; *Vigun07g219600*). (*C*) Cumulative RLU counts from *A* and *B* after indicated peptide treatments. Bars show average of $n = 8$ leaf discs ± SEM. (*D*) Receptor-dependent ethylene production in *N. benthamiana* after treatment with H_2O or 1 μM peptides. Bars show average of $n = 6$ leaf discs ± SEM. (*E*) *Vu*-In^{-A}/H_2O induced ethylene response ratio in select cowpea germplasm (*Top*), with corresponding ROS responses when INR alleles are expressed in *N. benthamiana* (*Bottom*). Gray boxes indicate accessions with GG allele at mapped marker 2_22561, and white boxes indicate AA allele. See *SI Appendix*, Table S2 for a full list of UCR Minicore responses. Bars show average of $n = 8$ leaf discs ± SEM. Within *C*–*E*, different letters indicate significant differences (all ANOVAs $P < 0.05$; Tukey HSD, $\alpha = 0.05$).

or *Glyma.10G228100*) enabled *Vu*-In–induced ethylene production (*SI Appendix*, Fig. S8). Soybean plants are both unresponsive to inceptin (11), and phylogenetic analysis of its four syntenic homologs showed that they fall outside the subclade of functional *INR* genes (*SI Appendix*, Fig. S8). We conclude that a subtribe of legume species, including *Phaseolus* and *Vigna*, uniquely encode functional INRs sufficient to confer HAMP-induced responses in tobacco.

In plants, LRR-RLPs can either directly bind ligands or can instead modulate the binding activities of other LRR-RKs (21, 22). Unlike modulating RLPs, which display clear orthologs across plant families and contain comparatively short ectodomains (23), INR shares structural and phylogenetic features common in *Arabidopsis* and tomato ligand-binding receptors (24–26), including a large ectodomain, an intervening motif (27), and membership in a large clade-specific gene family (*SI Appendix*, Fig. S10). Our data cannot exclude the presence of a latent INR endogenous to tobacco, which, upon activation by heterologous expression of *Vigun07g219600* or its homologs, allows *Vu*-In–induced responses. However, the most parsimonious model is that legume-specific perception of inceptin peptides is mediated by INR as a lineage-specific RLP.

To examine inceptin binding in vitro, INR was expressed heterologously in insect cells and purified, but interpretation was confounded by predominant aggregation of the protein product (*SI Appendix*, Fig. S11). As an alternative method to obtain support for in planta peptide binding activity to INR, we generated an N-terminal acridinium-tagged *Vu*-In conjugate and measured retention of luminescence signal by immunoprecipitated,

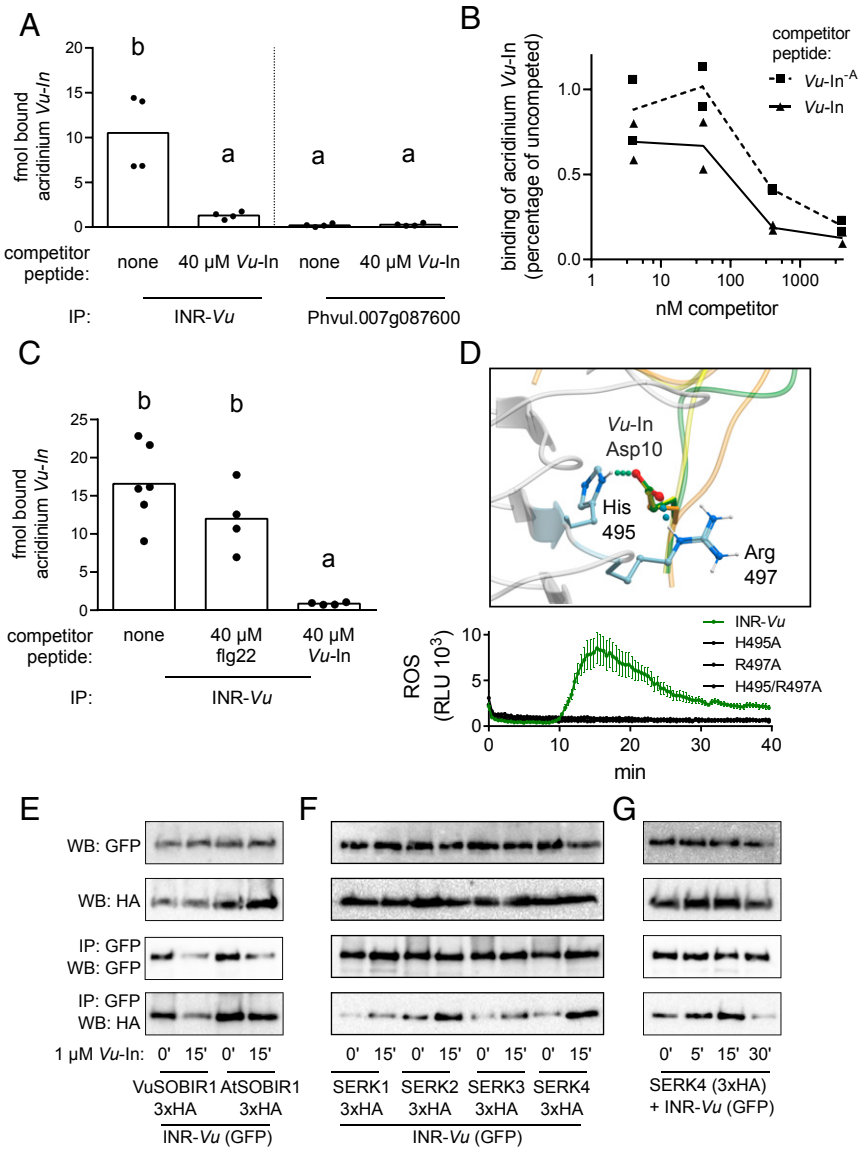

Fig. 3. INR confers acridinium-*Vu*-In retention and displays both constitutive and inducible coreceptor/adapter RLK associations. (*A*) Quantified acridinium-In retention to immunoprecipitated, GFP-tagged LRR-RLPs in the presence or absence of competitor peptide. (*B*) Competition curve of free *Vu*-In or *Vu*-In^{-A} peptide against 0.3 µM acri-In bound to immunoprecipitated INR-*Vu*. (*C*) *Vu*-In but not flg22 competes for peptide retention to immunoprecipitated INR-*Vu*. In *A*–*C*, points indicate replicate luminescence measurements. (*D*) Predicted binding site for *Vu*-In with His495 and Arg497 of INR-*Vu*. ROS production after 1 µM *Vu*-In treatment is shown for *N. benthamiana* leaf punches ($n = 8$) expressing INR-*Vu* (green) or mutant variants (black). (*E*–*G*) INR-*Vu* coimmunoprecipitates (IP) cowpea (*Vu*) and *Arabidopsis* (*At*) homologs of SOBIR1 and AtSERK RLKs(1-4). VuSOBIR1 (*Vigun09g096400*) or AtSOBIR1 (*AT2G31880*) were coexpressed with INR-*Vu*. (*D* and *E*) AtSERK1-4 were coexpressed with INR-*Vu*. All receptor (C-terminal GFP) and coreceptor (C-terminal 3xHA) combinations were expressed in *N. benthamiana*. Tissue was harvested after peptide infiltration at the time indicated 0-30m, 0-30′). Western blots (WB) were probed with either GFP or HA antibody. Representative results are shown from three independent experiments.

semipurified INR-GFP expressed in *N. benthamiana* leaves. Acri-*Vu*-In was similarly bioactive in eliciting ethylene release in cowpea (*SI Appendix*, Fig. S12). Immunoprecipitated INR-*Vu* retained an acridinium-*Vu*-In luminescent signal while an unrelated RLP control, Phvul.007g087600, showed no retained signal (Fig. 3*A*). Preincubation with unlabeled *Vu*-In, but not flg22, competed acridinium-derived signal, supportive of specific binding (Fig. 3 *A*–*C*). Both *Vu*-In and *Vu*-In^{-A} compete for acridinium-*Vu*-In retention at concentrations from 50 to 500 nM (Fig. 3*B*).

To better understand potential sites that could mediate direct physical interactions of INR with inceptin, we constructed a homology model of INR based on the crystal structure of the LRR ectodomain of FLAGELLIN-SENSING 2 (FLS2) (28) and performed *Vu*-In docking simulations. The predicted lowest energy conformations were ranked by peptide binding scores. In multiple low-energy conformations of *Vu*-In, the ligand acidic residue Asp10 showed a conserved binding position and conformation by interacting with both basic INR-*Vu* residues His495 and Arg497 (Fig. 3*D* and *SI Appendix*, Fig. S12). Consistent with a predicted role in binding, a previous Ala substitution study demonstrated that Asp10 was the only AA essential for *Vu*-In–elicited ethylene production (9). To examine the predicted interaction, we substituted INR-*Vu* at His495/Arg497 to Ala495/Ala497, which resulted in loss of both acridinium-*Vu*-In retention and *Vu*-In–induced ROS production in *N. benthamiana* (Fig. 3*D* and *SI Appendix*, Fig. S12). Substituted INR colocalized with plasma membrane marker PIP2A-mCherry (*SI Appendix*, Fig. S5) and was present in biochemical plasma membrane fraction (*SI Appendix*, Fig. S12). We further investigated the role of His495 and Arg497 through charge swap substitutions to Asp and Asp/Glu, respectively; however, these combinations were not sufficient to confer responsiveness to a respectively charge substituted *Vu*-In peptide (Asp10→Lys/Arg) (*SI Appendix*, Fig. S13). His495 and Arg497 are conserved in several *Vigna* and *Phaseolus* INR homologs, but not in nonfunctional soybean RLP homologs (*SI Appendix*, Fig. S14), consistent with a role in inceptin recognition with other conserved features of INR controlling signaling outputs. Our data show that INR-*Vu* is sufficient to confer acridinium-*Vu*-In retention in tobacco and that this activity is in part mediated by His495/Arg497.

Plant LRR-type surface receptors typically associate with somatic embryogenesis receptor kinase (SERK) coreceptors for signal transduction (29). In addition, characterized RLPs constitutively associate with the adapter RK Suppressor of BIR1 (SOBIR1) (30). We tested if INR associates with *Arabidopsis* and cowpea orthologs of SOBIR1 by coimmunoprecipitation (co-IP). Association of INR with both AtSOBIR1 and VuSOBIR1 (*Vigun09g096400*) was constitutive (Fig. 3*E*) while INR associated more strongly with AtSERK coreceptors after peptide treatment (Fig. 3 *F* and *G*). Likewise, the co-IP of SERKs requires INR (*SI Appendix*, Fig. S15). Thus, INR associates with coreceptor and adapter RKs in a manner similar to characterized LRR-RLPs.

To test if INR is sufficient to enhance antiherbivore defenses in plants lacking native inceptin responses, we stably transformed *N. benthamiana* and *Nicotiana tabacum* with either 35S:INR-*Vu* or 35S:INR-*Pv* transgenes. Multiple independent transgenic lines expressing 35S:INR responded to *Vu*-In, as measured by induced ethylene and induced peroxidase activity as a direct defense output (Figs. 4 *A* and *B* and *SI Appendix*, Fig. S16). Transcriptomic characterization of *Vu*-In–induced responses in *N. benthamiana* INR-*Pv* line 1-5 showed up-regulation of characteristic antiherbivore defense genes (*SI Appendix*, Fig. S17). We confirmed that two classical defense markers, a Kunitz trypsin inhibitor (KTI) (31) and ascorbate oxidase (AscOx) (32), were up-regulated in the presence of both INR and *Vu*-In application (Fig. 4*C* and *SI Appendix*, Fig. S18).

We challenged INR-expressing tobacco lines with second instar larvae of the generalist Lepidopteran herbivore, beet armyworm (*Spodoptera exigua*). Both *N. benthamiana* and *N. tabacum* harbor a substitution in the inceptin precursor cATPC (V256N), creating an *Nb*/*Nt*-In peptide upon proteolytic processing. We confirmed both the presence of *Nb*/*Nt*-In in *Spodoptera* OS after consumption of tobacco at similar levels to *Vu*-In, and the bioactivity of *Nb*/*Nt*-In on plants expressing INR-*Vu* (*SI Appendix*, Fig. S19). Consistent with INR enabling recognition of inceptin peptides, caterpillars displayed 32 to 37% lower relative growth rates (RGRs) on transgenic lines than on wild-type (WT) plants when caged on either *Nicotiana* species for 4 d (Fig. 4 *D* and *E*). A similar magnitude of caterpillar growth reduction was previously observed after pretreatment of cowpea with *Vu*-In (8). Our data support that the heterologous expression of either INR-*Vu* or INR-*Pv* can confer enhanced antiherbivore defense responses.

Discussion

Plant recognition of modified-self and nonself patterns enables increased resistance to diseases and pests (12). Immune recognition of specific PAMPs is often mediated by PRRs, but defined HAMP receptors have remained largely unknown. Here, we describe INR, an LRR-RLP family protein sufficient to confer signaling and defense responses to precisely defined HAMPs. Our work builds on previous findings implicating cell surface signaling elicited by HAMPs. Plant responses to specific HAMPs can be reduced when candidate receptors or downstream pathway components are silenced (33–36). Similarly, a fatty acid amide HAMP elicitor was shown to bind maize plasma membrane preparations (37). We demonstrate that INR confers retention of acridinium-*Vu*-In signal when expressed in tobacco (Fig. 3 *A*–*C*) and identify AA residues that mediate both signaling and acridinium-*Vu*-In retention (Fig. 3*D* and *SI Appendix*, Fig. S12). Collectively, our data are consistent with a role for INR as a defined HAMP receptor. Further technical advances in LRR in vitro biochemistry will be needed to generate additional support and evidence for direct INR–inceptin binding interactions.

INR is only found in certain nonmodel legume species and is consistent with lineage-specific HAMP perception in plant families (11). Our findings are consistent with the majority of demonstrated PRRs in the RLP gene family, which often belong to large lineage-specific clades (24). Consistent with a similar PRR function in legumes, we observed natural variation in strength of INR alleles (Fig. 2*E* and *SI Appendix*, Fig. S4), the restricted presence of functional INR homologs in select, *Vu*-In–responsive legume genomes (Fig. 2*A* and *SI Appendix*, Fig. S8), and shared structural and phylogenetic features of INR with demonstrated lineage-specific receptors (*SI Appendix*, Fig. S10). While a modeled binding site can be found in other RLP homologs at the locus, other conserved features are shared in the INR clade: for example, a truncated intracellular sequence (*SI Appendix*, Fig. S14) consistent with sensitive roles for this subdomain in effective RLP signaling (38). Demonstrating a precise requirement of *INR* for *Vu*-In response in legumes will require reliable reverse genetic tools in cowpea, currently limited by poor receptivity to transformation.

Inceptin peptides have been identified in the OS of all examined Lepidopteran species and are produced after feeding on a variety of host plant species (8, 10) (*SI Appendix*, Fig. S19). The receptor activity of INR is thus consistent with other plant PRRs recognizing conserved patterns associated with danger or attack (12). Despite similarity in peptide recognition as an immune strategy, responses to distinct peptide PAMPs can vary in genetic requirements (39), and defense outputs to herbivores differ from pathogen-induced responses (40, 41). INR now provides a genetic tool to define attacker-specific signaling pathways in plants.

Dynamic plant defense responses to herbivory have been examined for nearly 50 y (5, 31, 42–45). Our data provide support for a current working hypothesis and model where INR directly

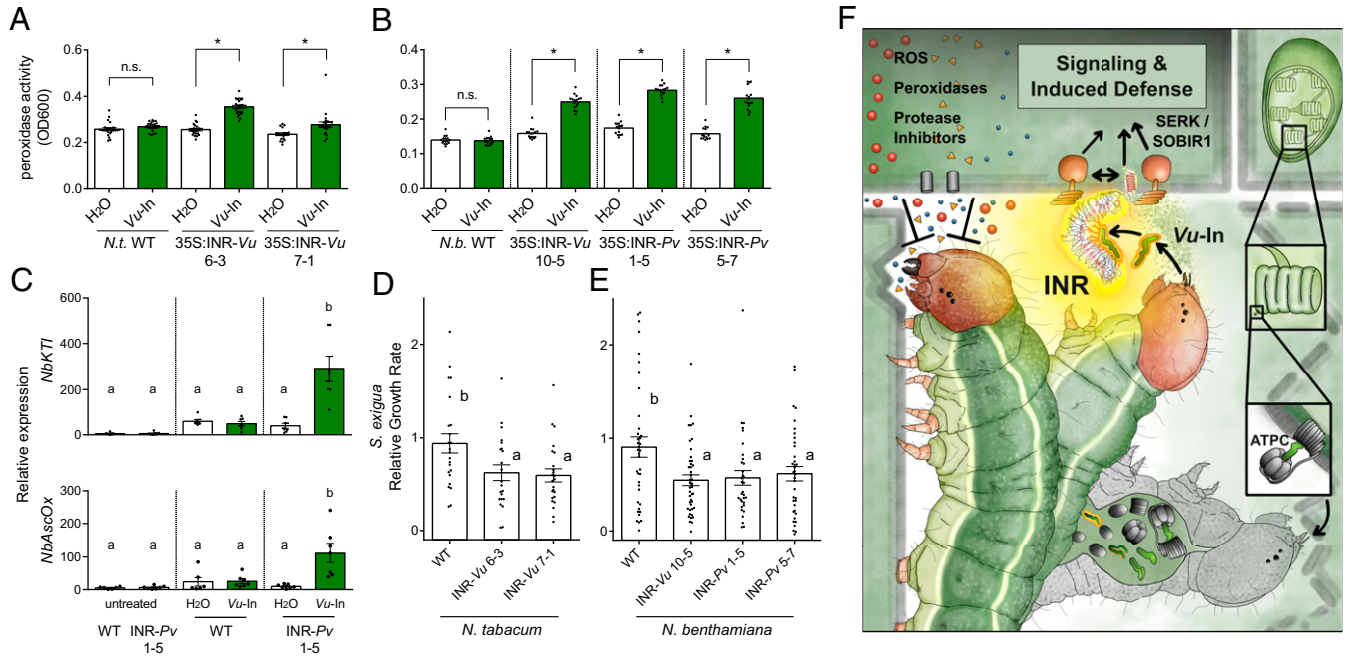

Fig. 4. Heterologous INR expression regulates inducible plant defenses and herbivore resistance in tobacco species. (*A* and *B*) *Vu*-In induces peroxidase activity in stable INR transgenic lines of *N. tabacum* (*N.t.*) and *N. benthamiana* (*N.b.*). Bars show average ± SEM of $n = 16$–24 leaf discs after incubation with 1 μM *Vu*-In. An asterisk (*) denotes statistical significance ($P < 0.05$ Student's *t* test), n.s. indicates no significant difference. (*C*) qPCR quantification of *Vu*-In–induced defense transcripts for a *Kunitz Trypsin Inhibitor* (*KTI*) and an *Ascorbate Oxidase* (*AscOx*) in 35S:INR-*Pv* transgenic *N. benthamiana* line 1-5. Relative expression of defense markers in $n = 6$–7 replicate plants are shown (see *SI Appendix*, Fig. S15 for additional details). (*D* and *E*) RGRs of beet armyworm (*S. exigua*) larvae reared on transgenic or WT lines of *N. tabacum* (*D*) and *N. benthamiana* (*E*). Bars show average of $n > 22$ *N. tabacum* plants from two independent experiments or $n > 33$ *N. benthamiana* plants from four independent experiments ± SEM, with individual dots showing individual larvae. Different letters indicate significantly different means (Tukey HSD, $\alpha = 0.05$). (*F*) Conceptual model of chewing herbivore recognition and induced defense elicitation in legumes via INR. Foliar attack by caterpillars on cowpea (*V. unguiculata*, Vu) results in gut proteolysis of chloroplastic ATP synthase-subunits (ATPCs) and the production of inceptin peptides, such as Vu-In, in OS. Subsequent bouts of herbivory stimulate recognition of Vu-In by INR, a legume-specific LRR-RLP. INR constitutively and dynamically associates with SOBIR1 and SERK (LRR-RLK) coreceptors, respectively. The collective outcome is the enhanced production of subsequent induced defense signals, such as ROS and ethylene, which in part contribute to the up-regulation of additional proteinaceous defenses. Inceptin-elicited production of direct defenses, such as peroxidases and trypsin inhibitors, is part of a complex array of biochemical changes that collectively suppress insect growth rates.

recognizes inceptin peptides via a plant immune network of adapters and coreceptors, mediating defense outputs (Fig. 4*F*). INR mediates plant defense in response to a common oral secretion pattern in Lepidoptera (10) and represents a functional immune surveillance module that can be imparted to nonlegume plant families. With pest invasions routinely threatening food security, a greater understanding of mechanisms underpinning plant–herbivore recognition is critical (44). More broadly, defined receptor–ligand pairs for plant–herbivore interactions are needed to provide essential mechanistic tools to understand and regulate interactions between autotrophs and animals.

Methods

Plant Materials and SNP Genotyping. *P. vulgaris* accession G19833 was kindly provided by Phil Miklas, US Department of Agriculture (USDA, Prosser, WA); accession Red Hawk was kindly provided by Jim Kelly, Michigan State University, East Lansing, MI; and *V. radiata* accession VC1973A ("Tex-Sprout") was kindly provided by Creighton Miller, Texas A&M University, College Station, TX. All other soybean and common bean germplasm was made available through the USDA Germplasm Resources Information Network (GRIN), specifically with invaluable assistance from the Western Regional Plant Introduction Station (Pullman, WA) and the Soybean Germplasm Collection (Urbana, IL).

Two populations were used for mapping of *Vu*-In^{-A} response: 85 lines from a biparental RIL population derived from a cross between Yacine and 58-77 that was developed previously (46), and a set of 364 cowpea accessions representing worldwide diversity of cultivated cowpea (17). Both populations were genotyped with the Cowpea iSelect Consortium Array containing 51,128 SNPs (18) at the University of Southern California Molecular Genomics Core facility (Los Angeles, CA). SNPs were called using GenomeStudio software (Illumina, Inc., San Diego, CA) with the custom file from Muñoz-Amatriaín et al. (18). Data curation was performed by removing SNPs with more than 20% missing or heterozygous calls.

Linkage and QTL Mapping. For linkage map construction, RILs with high heterozygosity and those carrying nonparental alleles were eliminated prior to mapping. Of the remaining 100 RILs, 17,638 SNPs that were polymorphic in both the parents and the RIL population, and that had minor allele frequencies (MAFs) >0.20 were used. MSTmap (47) (http://www.mstmap.org/) was used for genetic map construction, with the following parameters: grouping logarithm of odds criteria = 10; population type = doubled haploid (DH); no mapping size threshold = 2; no mapping distance threshold: 10 cM; try to detect genotyping errors = no; and genetic mapping function = kosambi. The linkage groups were numbered and oriented according to cowpea pseudomolecules (19). Since the DH function inflated the centimorgan distance for an RIL population, centimorgan distances were divided by two to correct for the extra round of effective recombination occurring in an RIL population compared to a DH population.

QTL analysis was performed using a linear mixed model described by Xu (48) and implemented in R following Lo et al. (49). A modified Bonferroni correction ($\alpha = 0.05$) that uses the effective number of markers or effective degrees of freedom instead of the total number of SNPs as a denominator was used to set the genome-wide critical value, as in Lo et al. (49). This set the significance cutoff to a $-\log_{10}(P \text{ value})$ of 4.84 for mapping *Vu*-In^{-A} response.

GWAS. The GWAS was performed in a panel of UCR Minicore accessions (*SI Appendix*, Table S2) using the mixed linear model (MLM) function (50) implemented in TASSEL v5 (https://www.maizegenetics.net/tassel), with a principal component analysis (five principal components) accounting for

population structure in the dataset and a kinship matrix correcting for genetic relatedness between accessions. A total of 42,686 SNPs with MAF of >0.05 were used for GWAS. SNPs were ordered based on their physical position in the cowpea reference genome (19). A false discovery rate (α = 0.05) was used for multiple testing correction of the GWAS results, which set the significance threshold to a $-\log_{10}(P$ value) of 3.93 for mapping *Vu*-In^{-A} response.

Peptide-Induced Ethylene Production. Inceptin peptides based on *V. unguiculata* cATPC sequence, *Vu*-In (ICDINGVCVDA) and *Vu*-In^{-A} (ICDINGVCVD), were synthesized (Genscript) and reconstituted in H_2O. Induced ethylene accumulation in cowpea or common bean was measured in first fully extended trifoliate leaves of 3-wk-old greenhouse-grown seedlings, grown from March to November in San Diego, CA in 3.5-inch pots using commercial potting soil (Berger Mix 2) supplemented with 5 mL of Florikan 18-5-12. Leaflets were lightly scratch-wounded in each corner with a fresh razor blade to remove cuticle over an area of 1 cm^2, and 10 μL of H_2O with or without peptide was equally spread over the four wounds with a pipette tip. After 1 h, leaflets were excised and placed in sealed tubes for 1 h before headspace sampling. Ethylene was measured by gas chromatography using a short 1-m column (13018-U, 80/100 μm Hayesep Q; Supelco) with flame ionization detection and quantified using a standard curve following Schmelz et al. (51). The experimental design for forward genetic studies using ethylene as a response output was as follows: Two plants of each of 85 RILs were treated with H_2O or *Vu*-In^{-A} as described above, on paired leaflets of either trifoliate or primary leaves. The ratio of ethylene production per gram of tissue (*Vu*-In^{-A}:H_2O) was calculated for each individual pair of leaflets, and the log-corrected average of the four pairs was used for QTL mapping. For GWAS, experimental design was similar, except one trifoliate leaf of a single seedling of each of 364 lines was treated.

For ethylene assays in *N. benthamiana*, plants were grown in Berger Mix 2 with weekly supplemental fertilizer in a growth room (12 h light, 150 μmol·m^{-2}·s^{-1}) at 22 °C. A recent fully expanded leaf of 4-wk-old plants was infiltrated with a blunt syringe and patted dry with a paper towel, and four leaf discs within the infiltrated area were immediately excised with a no. 5 cork borer and sealed in tubes. Headspace ethylene was measured after 3 h of accumulation.

Molecular Cloning and Transient and Stable Expression. Full-length complementary DNA (cDNA) sequences of all described receptors and coreceptors were PCR amplified using primers (*SI Appendix*, Table S2) from 5′ SMARTer RACE cDNA libraries (Takara Biosciences). Unless otherwise noted, INR-*Vu* and INR-*Pv* indicate the genes or protein products of *Vigun07g219600.1* and *Phvul.007g077500.1*, obtained from reference sequenced accessions IT97K-499-35 and G19833, respectively. All other genes were cloned from reference accessions Tex-Sprout (*V. radiata*) and Williams 82 (*G. max*). For the highly similar soybean genes *Glyma.10G228000* and *Glyma.10G228100*, a larger fragment was subcloned from genomic DNA using primers with local homology for flanking sequences on chromosome 10; then, a single primer pair was used to amplify either coding sequence. Amplicons were inserted using Gateway technology (Invitrogen) into plant expression vectors pEarleyGate103 (52) for C-terminal GFP or pGWB414 (53) for C-terminal 3xHA tag. Constructs were electroporated into *Agrobacterium tumefaciens* strain GV3101 (pMP90) (54). Agrobacterium strains for expression of individual constructs were induced with 150 μM acetosyringone in 10 mM 2-(*N*-morpholino)ethanesulfonic acid (MES), pH 5.6, 10 mM $MgCl_2$ and infiltrated into *N. benthamiana* leaves at optical density at 600 nm (OD_{600}) of 0.45. Western blotting was performed with α-GFP polyclonal (A-6455; Thermo) or α-hemagglutinin (α-HA) monoclonal (clone HA-7, H3663; Sigma) primary antibodies at 1:1,000 dilution, and α-rabbit (A6154; Sigma) or α-mouse (A4416; Sigma) secondary antibodies at 1:10,000 dilution. Transgenic lines of *N. benthamiana* and *N. tabacum* var. SR1 were obtained from the University of California, Davis Plant Transformation Facility using GV3101 strains (pEG103) with INR-*Vu* or INR-*Pv* (C-terminal GFP) inserts. T1 lines with segregation of glufosinate resistance consistent with single transgene insertions were selfed, and homozygous T2 lines were selected.

Ectodomain Expression and Purification. The INR-*Vu* (residues 23 to 845) coding sequence was subcloned in a modified pFastBac vector (Geneva Biotech) containing the *Drosophila* immunoglobulin heavy chain binding protein signal peptide, a C-terminal tobacco etch virus (TEV) cleavable StrepII–10x His tag and noncleavable Avi-tag (55, 56). *Trichoplusia ni* (strain Tnao38) (57) cells were infected with a multiplicity of infection (MOI) of 5 at a density of 2×10^6 cells per milliliter and incubated for 26 h at 28 °C and for an additional 46 h at 22 °C. The secreted protein was purified from supernatant by Ni^{2+} (HisTrap Excel; GE Healthcare) (equilibrated in 50 mM potassium phosphate, pH 7.6, 250 mM NaCl, 1 mM 2-mercaptoethanol) and StrepII (Strep-Tactin XT Superflow high affinity chromatography; IBA) (equilibrated in 20 mM Tris, pH 8.0, 250 mM NaCl, 1 mM ethylenediaminetetraacetic acid [EDTA]) affinity chromatography. Proteins were then dialyzed in 20 mM sodium citrate, pH 5.0, 250 mM NaCl for 3 h and further purified by size-exclusion chromatography on a HiLoad 26/600 Superdex 200 pg column (GE Healthcare), equilibrated in 20 mM sodium citrate, pH 5.0, 250 mM NaCl. Monomeric peak fractions were dialyzed in 50 mM Tris, pH 8.0, 250 mM NaCl, 1 mM 2-mercaptoethanol, and the tag was cleaved with TEV protease at 4 °C overnight and removed by size-exclusion chromatography on a Superdex 200 increase 10/300 GL column (GE Healthcare), equilibrated in 20 mM sodium citrate, pH 5.0, 250 mM NaCl.

Biotinylation and Grating-Coupled Interferometry. INR-*Vu* ectodomain was biotinylated with biotin ligase BirA (2 μM) (56) for 1 h at 25 °C, in a volume of 200 μL; 25 mM Tris, pH 8, 150 mM NaCl, 5 mM $MgCl_2$, 2 mM 2-mercaptoethanol, 0.15 mM biotin, 2 mM ATP, followed by size-exclusion chromatography to purify the biotinylated protein. Binding kinetic measurements were performed with the Creoptix WAVE system (Creoptix AG) using 4PCP chips (thin quasiplanar polycarboxylate surface) (Creoptix AG). Chips were conditioned with borate buffer (100 mM sodium borate, pH 9.0, 1 M NaCl) (Xantec), and streptavidin (20 μg·ml^{-1}) (Sigma) was immobilized on the chip surface using amine-coupling; activation [1:1 mix of 400 mM *N*-(3-dimethylaminopropyl)-*N*′-ethylcarbodiimide hydrochloride and 100 mM *N*-hydroxysuccinimide] (Xantec) was for 7 min, followed by injection of streptavidin in 10 mM sodium acetate, pH 5.0 (Sigma), until the desired density was reached, passivation of the surface (0.5% bovine serum albumin [Roche] in 10 mM sodium acetate, pH 5.0) for 10 min, and final quenching with 1 M ethanolamine, pH 8.0 (Xantec) for 7 min. Biotinylated INR-*Vu* ectodomain (10 μg·ml^{-1}) was captured on the streptavidin-coupled chip surface until the desired density was reached. Kinetic analyses were performed at 25 °C with a 1:2 dilution series from 10 μM in 20 mM citrate, pH 5.0, 250 mM NaCl, 0.01% Tween 20. Blank injections were used for double referencing and a dimethyl sulfoxide (DMSO) calibration curve for bulk correction. Analysis and correction of the obtained data were performed using the Creoptix WAVE control software (correction applied: X and Y offset; DMSO calibration; double referencing).

Homology Modeling of INR-*Vu* and Docking of *Vu*-In. The crystal structure of the LRR ectodomain of FLS2 (Protein Data Bank [PDB] ID code 4MN8) was used as the template. The sequence of INR-*Vu* was aligned with the sequence of the template through the zero end-gap global alignment (ZEGA) method with the Gonnet comparison matrix (58, 59). The penalty of gap opening and extension was set as 2.4 and 0.15, respectively. Based on the alignment and template structure, a homology model of INR-*Vu* was built with the homology modeling tool and default parameters in ICM-Pro (60). All side chains and insertions/deletions were refined via a biased probability Monte Carlo (BPMC) sampling (61)

The cocrystallized 22-AA peptide in the crystal structure template (PDB ID code 4MN8) was used to define the docking region. A set of potential maps were generated for the docking region on a 0.5-Å three-dimensional grid, containing 1) van der Waals interaction, 2) electrostatic interaction, 3) hydrogen bond, and 4) hydrophobic potential grids. With potential maps, docking and scoring of *Vu*-In were performed using a stochastic global energy optimization procedure in internal coordinates implemented in the ICM-Pro v3.8-6a (62), described as the following steps. 1) The *Vu*-In peptide was sampled with the implicit solvation model to generate a series of starting conformations via the BPMC method, and each starting conformation was placed into the docking region with four principal orientations. 2) *Vu*-In was sampled in the precalculated potential maps through BPMC sampling to optimize its positional and internal variables. 3) After sampling, 10 top ranking conformations were rescored with the internal coordinate mechanics (ICM) full atom scoring function, and conformations were resorted by the docking score.

Acridinium-Labeled Peptide. Acridinium-labeled *Vu*-In (acri-In) was synthesized using *N*-hydroxy-succinimidyl (NHS) acridinium ester (Cayman Chemical) quenched with Tris, pH 8, and purified by reverse phase high performance liquid chromatography (HPLC) (Poroshell 120 EC-C18; Agilent) by tracking absorbance at 372 nm. Final labeled peptide concentration was determined using a standard curve of absorbance of the NHS-acridinium standard.

Acridinium retention assays were performed according to Butenko et al. (63) and Wang et al. (64) with modification. Protein was extracted from 1 g

of *N. benthamiana* tissue expressing RLP genes (48 hours post-infiltration Agrobacterium), using a solution of 50 mM Tris, pH 7.5, 150 mM NaCl, 1% Nonidet P-40, 10% glycerol, 1 mM phenylmethylsulfonyl fluoride (PMSF), and 1× Roche Protease Inhibitor Mixture. Homogenized extracts were cleared for 30m, 20,000 relative centrifugal force (rcf), and the supernatant was then incubated with end-over-end mixing with 10 μL of GFP-Trap MA resin (Chromotek) for 3 h. The immunoprecipitated receptor was washed twice in extraction buffer (1 mL) and twice in binding buffer (1 mL per wash, 50 mM Tris, pH 7.5, 150 mM NaCl, 1 mM PMSF). Immunoprecipitates were aliquotted using 80 μL per replicate tube. Four microliters of either H_2O or excess competitor peptide was added, to a final concentration of 4 nm-40 μM, and the preparation was preincubated on ice for 2 h. Acri-In in binding buffer was added to a final concentration of 200 nM with or without additional competitor peptide (final concentration 80 μM in 100 μL volume). After 20 min incubation on ice with occasional mixing, pellets were washed twice with 1 mL of binding buffer and resuspended in 100 μL of 5 mM citric acid. Pellet-retained luminescence was measured using a Biotek Synergy H2 Multimode plate reader by injecting 100 μL of trigger buffer (0.2 N NaOH, 0.1% H_2O_2) and reading 10-s luminescence, and a standard curve of acri-In was used to determine retained peptide concentration.

Coimmunoprecipitation of Coreceptor and Adapter Kinases. Following *Agrobacterium* infiltration (48 h), *N. benthamiana* leaves expressing both INR or EFR (C-terminal GFP) and SOBIR1 or SERKs (C-terminal 3xHA) were infiltrated with peptide solutions and harvested on liquid N_2 at specified time points. Tissue was ground on an N_2-chilled mortar and pestle and homogenized in 2 $mL \cdot g^{-1}$ extraction buffer (50 mM Tris, pH 7.5, 150 mM NaCl, 1% Nonidet P-40, 10 mM dithiothreitol, 1× Roche Protease Inhibitor) and then cleared by centrifugation (30 m, 20,000 rcf). Supernatant was incubated with 10 μL of GFP-Trap A beads (Chromotek) by end-over-end mixing at 4 °C and eluted in 30 μL of Laemmli buffer (95 °C, 5 min).

Plasma Membrane Purification. *N. benthamiana* tissue expressing INR-*Vu* or mutant receptor was homogenized in lysis buffer (0.33 M sucrose, 50 mM Tris, pH 7.5, 5 mM EDTA, 1× Roche Protease Inhibitor) and cleared by centrifugation (10′, 6,000 rcf), and the supernatant was filtered through Miracloth. Membranes were pelleted by ultracentrifugation (30′, 100,000 rcf). Membranes were resuspended in resuspension buffer (0.33 M sucrose, 5 mM KPO_4, pH 7.8, 3 mM KCl, 1× Roche Protease Inhibitor) and separated in a two-phase solution of 6.2% Dextran T500 and polyethylene glycol (PEG) 3350. Upper and lower phases were pelleted by ultracentrifugation to yield plasma membrane and microsomal fractions, respectively (65). Total protein was quantified by bicinchoninic acid (BCA) assay (Thermo) and equal protein was loaded for Western blotting.

ROS Production and Peroxidase Activity Assays. Following *Agrobacterium* infiltration for receptor expression (24 h), leaf punches were taken with a 4-mm biopsy punch and floated in 50 μL of H_2O using individual cells of a white 96-well plate. After overnight incubation, ROS production was measured using luminol-horseradish peroxidase (HRP) over 40 min as described (66) using a Biotek Synergy H2 Multimode plate reader. Peroxidase activity was measured as described by Mott et al. (67) with the following modifications. Leaf discs were taken from fully extended leaves of 4-wk-old *Nicotiana* seedlings, washed for 1 h in 1/2 (half-strength) Murashige Skoog (MS) salt ($4.4\ g \cdot L^{-1}$), and incubated overnight in 1/2 MS with 1 μM peptide prior to reaction with 5-aminosalicylic acid.

Transcriptomic and qPCR Analysis. *N. benthamiana* stable transgenic line expressing *P. vulgaris* INR (INR-Pv 1-5) was syringe infiltrated with H_2O or 1 μM *Vu*-In, and total leaf tissue was harvested 6 h later. Total RNA was extracted using a Nucleospin Plant RNA kit (Macherey-Nagel). RNA was used to generate Lexogen Quantseq 3′ RNA seq libraries at the Cornell University Institute of Biotechnology Genomics Facility. The 3′ reads were mapped to *N. benthamiana* genome v1.0.1 (Sol Genomics Network) using HISAT2 (68), counts by gene were analyzed using HTSeq-Count (69), and differential expression was analyzed by DESeq2 (70).

Highly *Vu*-In up-regulated genes relative to H_2O-infiltrated tissue were prioritized for qPCR analysis. In replicated experiments, plant material was treated as before in the transcriptome analysis, and cDNA libraries were generated using SuperScript III (Life Technologies). qPCR was performed using primers in *SI Appendix*, Table S2.

Measurement of Inceptin Peptides in OS. OS was collected from fourth instar *Spodoptera frugiperda* caterpillars that had fed for 48 h on leaves of defined host plants (*V. unguiculata*, *N. tabacum*, and *N. benthamiana*). Stable isotope internal standard-based quantification of OS inceptin levels, following Schmelz et al. (8), was obtained using ultra-high performance liquid chromatography-tandem mass spectrometry (UHPLC-MS/MS). Aliquots of 25 μL of spit were extracted on Oasis hydrophilic-lipophilic balance (HLB) cartridges (30 mg Oasis HLB; Waters, Milford, MA), evaporated, and reconstituted in 200 μL of 35% methanol for injection. The peptide separation was achieved on a Cortecs C18 column (100 mm length × 2.1 mm inside diameter, 1.6 μm) (Waters) using formic acid 0.05% in H_2O and acetonitrile as mobile phases. Detection was performed in electrospray positive ionization using the doubly charged ions $[M+2H]^{2+}$ as precursor ions for the multiple reaction monitoring (MRM) transitions, using selected MRM transitions 567.9 > 205.2, 492.2, 501.0 for 11-mer tobacco inceptin (*Nb*/*Nt*-In), 560.3 > 205.2, 493.1 for 11-mer cowpea inceptin (*Vu*-In), and 563.4 > 205.2, 304.2, 495.9 for the labeled internal standard. Data are from three independent replicates.

Herbivory Assays. Beet armyworm (*S. exigua*) larvae were obtained from Benzon (Carlisle, PA) as neonates and incubated at 28 °C for 48 h, and newly molted second instars were selected, preweighed, and placed on individual 3-wk-old plants. Each plant was contained with individual larvae using poly(vinyl chloride) cages secured at the base with surrounding potting soil. After 4 d, larvae were reweighed, and RGR was calculated (71).

Data Availability. Transcriptomic data are available at the National Center for Biotechnology Information Sequence Read Archive (submission no. PRJNA639603). All other study data are included in the article and *SI Appendix*.

ACKNOWLEDGMENTS. We thank Harley Riggleman, Ei Phu Lin, Behzad Maher, and Nile J. Hodges for technical assistance. We thank Yezhang Ding, Elly Poretsky, Keini Dressano, and Philipp Weckwerth for advice and discussions. We thank Michael Hothorn for providing facilities and guidance on in vitro biochemistry. Additional *P. vulgaris* germplasm was kindly provided by the USDA GRIN. A.D.S. was partially supported by E.A.S. and A.H. University of California San Diego (UC San Diego) startup funds, the Life Sciences Research Foundation, the University of California President's Postdoctoral Fellowship Program, a short-term European Molecular Biology Organization Postdoctoral Fellowship, and funding as a Washington Research Foundation Distinguished Investigator. E.A.S. and A.H. acknowledge partial support from the UC San Diego startup funds. Genotyping of cowpea accessions was supported by the Feed the Future Innovation Laboratory for Climate Resilient Cowpea (US Agency for International Development Cooperative Agreement AID-OAA-A-13-00070). OS analyses were supported by European Research Council Advanced Grant 788949. Research in the C.Z. laboratory was supported by The Gatsby Charitable Foundation and the Biotechnology and Biological Research Council (BB/P012574/1).

1. E. Stokstad, New crop pest takes Africa at lightning speed. *Science* **356**, 473–474 (2017).
2. M. E. Gray, T. W. Sappington, N. J. Miller, J. Moeser, M. O. Bohn, Adaptation and invasiveness of western corn rootworm: Intensifying research on a worsening pest. *Annu. Rev. Entomol.* **54**, 303–321 (2009).
3. E. C. Oerke, Crop losses to pests. *J. Agric. Sci.* **144**, 31–43 (2006).
4. R. Karban, I. T. Baldwin, *Induced Responses to Herbivory* (University of Chicago Press, 2007).
5. G. A. Howe, G. Jander, Plant immunity to insect herbivores. *Annu. Rev. Plant Biol.* **59**, 41–66 (2008).
6. E. A. Schmelz, Impacts of insect oral secretions on defoliation-induced plant defense. *Curr. Opin. Insect Sci.* **9**, 7–15 (2015).
7. H. T. Alborn *et al.*, An elicitor of plant volatiles from beet armyworm oral secretion. *Science* **276**, 945–949 (1997).
8. E. A. Schmelz *et al.*, Fragments of ATP synthase mediate plant perception of insect attack. *Proc. Natl. Acad. Sci. U.S.A.* **103**, 8894–8899 (2006).
9. E. A. Schmelz, S. LeClere, M. J. Carroll, H. T. Alborn, P. E. A. Teal, Cowpea chloroplastic ATP synthase is the source of multiple plant defense elicitors during insect herbivory. *Plant Physiol.* **144**, 793–805 (2007).
10. E. A. Schmelz *et al.*, An amino acid substitution inhibits specialist herbivore production of an antagonist effector and recovers insect-induced plant defenses. *Plant Physiol.* **160**, 1468–1478 (2012).
11. E. A. Schmelz, J. Engelberth, H. T. Alborn, J. H. Tumlinson III, P. E. A. Teal, Phytohormone-based activity mapping of insect herbivore-produced elicitors. *Proc. Natl. Acad. Sci. U.S.A.* **106**, 653–657 (2009).
12. A. A. Gust, R. Pruitt, T. Nürnberger, Sensing danger: Key to activating plant immunity. *Trends Plant Sci.* **22**, 779–791 (2017).
13. D. Couto, C. Zipfel, Regulation of pattern recognition receptor signalling in plants. *Nat. Rev. Immunol.* **16**, 537–552 (2016).
14. J. D. G. Jones, J. L. Dangl, The plant immune system. *Nature* **444**, 323–329 (2006).

15. C. Pfund *et al*., Flagellin is not a major defense elicitor in Ralstonia solanacearum cells or extracts applied to Arabidopsis thaliana. *Mol. Plant Microbe Interact.* **17**, 696–706 (2004).
16. U. Fürst *et al*., Perception of Agrobacterium tumefaciens flagellin by FLS2^{XL} confers resistance to crown gall disease. *Nat. Plants* **6**, 22–27 (2020).
17. S. Lo *et al*., A genome-wide association and meta-analysis reveal regions associated with seed size in cowpea [Vigna unguiculata (L.) Walp]. *Theor. Appl. Genet.* **132**, 3079–3087 (2019).
18. M. Muñoz-Amatriaín *et al*., Genome resources for climate-resilient cowpea, an essential crop for food security. *Plant J.* **89**, 1042–1054 (2017).
19. S. Lonardi *et al*., The genome of cowpea (Vigna unguiculata [L.] Walp.). *Plant J.* **98**, 767–782 (2019).
20. C. Zipfel *et al*., Perception of the bacterial PAMP EF-Tu by the receptor EFR restricts Agrobacterium-mediated transformation. *Cell* **125**, 749–760 (2006).
21. G. Lin *et al*., A receptor-like protein acts as a specificity switch for the regulation of stomatal development. *Genes Dev.* **31**, 927–938 (2017).
22. E. Holzwart *et al*., A mutant allele uncouples the brassinosteroid-dependent and independent functions of BRASSINOSTEROID INSENSITIVE 1. *Plant Physiol.* **182**, 669–678 (2020).
23. G. Wang *et al*., A genome-wide functional investigation into the roles of receptor-like proteins in Arabidopsis. *Plant Physiol.* **147**, 503–517 (2008).
24. P. A. Jamieson, L. Shan, P. He, Plant cell surface molecular cypher: Receptor-like proteins and their roles in immunity and development. *Plant Sci.* **274**, 242–251 (2018).
25. I. Albert, L. Zhang, H. Bemm, T. Nürnberger, Structure-function analysis of immune receptor AtRLP23 with its ligand nlp20 and coreceptors AtSOBIR1 and AtBAK1. *Mol. Plant. Microbe. Interact.* **32**, 1038–1046 (2019).
26. V. Hegenauer *et al*., Detection of the plant parasite Cuscuta reflexa by a tomato cell surface receptor. *Science* **353**, 478–481 (2016).
27. N. Matsushima, H. Miyashita, Leucine-rich repeat (LRR) domains containing intervening motifs in plants. *Biomolecules* **2**, 288–311 (2012).
28. Y. Sun *et al*., Structural basis for flg22-induced activation of the Arabidopsis FLS2-BAK1 immune complex. *Science* **342**, 624–628 (2013).
29. X. Ma, G. Xu, P. He, L. Shan, SERKing coreceptors for receptors. *Trends Plant Sci.* **21**, 1017–1033 (2016).
30. T. W. H. Liebrand *et al*., Receptor-like kinase SOBIR1/EVR interacts with receptor-like proteins in plant immunity against fungal infection. *Proc. Natl. Acad. Sci. U.S.A.* **110**, 10010–10015 (2013).
31. T. R. Green, C. A. Ryan, Wound-induced proteinase inhibitor in plant leaves: A possible defense mechanism against insects. *Science* **175**, 776–777 (1972).
32. G. W. Felton, C. B. Summers, Potential role of ascorbate oxidase as a plant defense protein against insect herbivory. *J. Chem. Ecol.* **19**, 1553–1568 (1993).
33. P. A. Gilardoni, C. Hettenhausen, I. T. Baldwin, G. Bonaventure, Nicotiana attenuata lectin receptor kinase1 suppresses the insect-mediated inhibition of induced defense responses during Manduca sexta herbivory. *Plant Cell* **23**, 3512–3532 (2011).
34. J. Wu, C. Hettenhausen, S. Meldau, I. T. Baldwin, Herbivory rapidly activates MAPK signaling in attacked and unattacked leaf regions but not between leaves of Nicotiana attenuata. *Plant Cell* **19**, 1096–1122 (2007).
35. T. Uemura *et al*., Soy and Arabidopsis receptor-like kinases respond to polysaccharide signals from Spodoptera species and mediate herbivore resistance. *Commun. Biol.* **3**, 224 (2020).
36. L. Hu *et al*., OsLRR-RLK1, an early responsive leucine-rich repeat receptor-like kinase, initiates rice defense responses against a chewing herbivore. *New Phytol.* **219**, 1097–1111 (2018).
37. C. L. Truitt, H.-X. Wei, P. W. Paré, A plasma membrane protein from Zea mays binds with the herbivore elicitor volicitin. *Plant Cell* **16**, 523–532 (2004).
38. A. K. Jehle *et al*., The receptor-like protein ReMAX of Arabidopsis detects the microbe-associated molecular pattern eMax from Xanthomonas. *Plant Cell* **25**, 2330–2340 (2013).
39. W.-L. Wan *et al*., Comparing Arabidopsis receptor kinase and receptor protein-mediated immune signaling reveals BIK1-dependent differences. *New Phytol.* **221**, 2080–2095 (2019).
40. J. Lazebnik, E. Frago, M. Dicke, J. J. A. van Loon, Phytohormone mediation of interactions between herbivores and plant pathogens. *J. Chem. Ecol.* **40**, 730–741 (2014).
41. C. M. J. Pieterse, D. Van der Does, C. Zamioudis, A. Leon-Reyes, S. C. M. Van Wees, Hormonal modulation of plant immunity. *Annu. Rev. Cell Dev. Biol.* **28**, 489–521 (2012).
42. T. C. Turlings, J. H. Tumlinson, W. J. Lewis, Exploitation of herbivore-induced plant odors by host-seeking parasitic wasps. *Science* **250**, 1251–1253 (1990).
43. M. Dicke, M. W. Sabelis, How plants obtain predatory mites as bodyguards. *Neth. J. Zool.* **38**, 148–165 (1988).
44. M. Erb, P. Reymond, Molecular interactions between plants and insect herbivores. *Annu. Rev. Plant Biol.* **70**, 527–557 (2019).
45. M. C. Schuman, I. T. Baldwin, The layers of plant responses to insect herbivores. *Annu. Rev. Entomol.* **61**, 373–394 (2016).
46. W. Muchero *et al*., A consensus genetic map of cowpea [Vigna unguiculata (L) Walp.] and synteny based on EST-derived SNPs. *Proc. Natl. Acad. Sci. U.S.A.* **106**, 18159–18164 (2009).
47. Y. Wu, P. R. Bhat, T. J. Close, S. Lonardi, Efficient and accurate construction of genetic linkage maps from the minimum spanning tree of a graph. *PLoS Genet.* **4**, e1000212 (2008).
48. S. Xu, Mapping quantitative trait loci by controlling polygenic background effects. *Genetics* **195**, 1209–1222 (2013).
49. S. Lo *et al*., Identification of QTL controlling domestication-related traits in cowpea (Vigna unguiculata L. Walp). *Sci. Rep.* **8**, 6261 (2018).
50. Z. Zhang *et al*., Mixed linear model approach adapted for genome-wide association studies. *Nat. Genet.* **42**, 355–360 (2010).
51. E. A. Schmelz, H. T. Alborn, E. Banchio, J. H. Tumlinson, Quantitative relationships between induced jasmonic acid levels and volatile emission in Zea mays during Spodoptera exigua herbivory. *Planta* **216**, 665–673 (2003).
52. K. W. Earley *et al*., Gateway-compatible vectors for plant functional genomics and proteomics. *Plant J.* **45**, 616–629 (2006).
53. Y. Tanaka *et al*., "Gateway vectors for plant genetic engineering: Overview of plant vectors, application for bimolecular fluorescence complementation (BiFC) and multigene construction" in *Genetic Engineering–Basics, New Applications and Responsibilities*, H. Barrera-Saldaa, Ed. (InTech, 2012), pp. 35–38.
54. C. Koncz *et al*., "Specialized vectors for gene tagging and expression studies" in *Plant Molecular Biology Manual*, S. B. Gelvin, R. A. Schilperoort, Eds. (Springer Netherlands, 1994), pp. 53–74.
55. M. G. Cull, P. J. Schatz, Biotinylation of proteins in vivo and in vitro using small peptide tags. *Methods Enzymol.* **326**, 430–440 (2000).
56. M. Fairhead, M. Howarth, Site-specific biotinylation of purified proteins using BirA. *Methods Mol. Biol.* **1266**, 171–184 (2015).
57. Y. Hashimoto, S. Zhang, G. W. Blissard, Ao38, a new cell line from eggs of the black witch moth, Ascalapha odorata (Lepidoptera: Noctuidae), is permissive for AcMNPV infection and produces high levels of recombinant proteins. *BMC Biotechnol.* **10**, 50 (2010).
58. R. A. Abagyan, S. Batalov, Do aligned sequences share the same fold? *J. Mol. Biol.* **273**, 355–368 (1997).
59. G. H. Gonnet, M. A. Cohen, S. A. Benner, Exhaustive matching of the entire protein sequence database. *Science* **256**, 1443–1445 (1992).
60. T. Cardozo, M. Totrov, R. Abagyan, Homology modeling by the ICM method. *Proteins* **23**, 403–414 (1995).
61. R. Abagyan, M. Totrov, Biased probability Monte Carlo conformational searches and electrostatic calculations for peptides and proteins. *J. Mol. Biol.* **235**, 983–1002 (1994).
62. R. Abagyan, M. Totrov, D. Kuznetsov, ICM—A new method for protein modeling and design: Applications to docking and structure prediction from the distorted native conformation. *J. Comput. Chem.* **15**, 488–506 (1994).
63. M. A. Butenko *et al*., Tools and strategies to match peptide-ligand receptor pairs. *Plant Cell* **26**, 1838–1847 (2014).
64. L. Wang *et al*., The systemin receptor SYR1 enhances resistance of tomato against herbivorous insects. *Nat. Plants* **4**, 152–156 (2018).
65. A. Lund, A. T. Fuglsang, Purification of plant plasma membranes by two-phase partitioning and measurement of H+ pumping. *Methods Mol. Biol.* **913**, 217–223 (2012).
66. J. M. Smith, A. Heese, Rapid bioassay to measure early reactive oxygen species production in Arabidopsis leave tissue in response to living Pseudomonas syringae. *Plant Methods* **10**, 6 (2014).
67. G. A. Mott, D. Desveaux, D. S. Guttman, A high-sensitivity, microtiter-based plate assay for plant pattern-triggered immunity. *Mol. Plant Microbe Interact.* **31**, 499–504 (2018).
68. D. Kim, J. M. Paggi, C. Park, C. Bennett, S. L. Salzberg, Graph-based genome alignment and genotyping with HISAT2 and HISAT-genotype. *Nat. Biotechnol.* **37**, 907–915 (2019).
69. S. Anders, P. T. Pyl, W. Huber, HTSeq–A Python framework to work with high-throughput sequencing data. *Bioinformatics* **31**, 166–169 (2015).
70. M. I. Love, W. Huber, S. Anders, Moderated estimation of fold change and dispersion for RNA-seq data with DESeq2. *Genome Biol.* **15**, 550 (2014).
71. G. P. Waldbauer, "The consumption and utilization of food by insects" in *Advances in Insect Physiology*, J. W. L. Beament, J. E. Treherne, V. B. Wigglesworth, Eds. (Academic Press, 1968), pp. 229–288.